Supplemental Material

Materials and Methods

DNA Preparation. Mature mouse TFAM was cloned into the pGEX-4T1 plasmid (GE Healthcare) after amplification using primers TFAM 5' end BamHI (attccgaagggatcctccagcatgggtagctatc) and TFAM 3' end XhoI (actccgtctctcgagttaatgctcagagatgtc) followed by sequence verification. Control region and COXI sequences were amplified using Control Region-99 bp Biotin-5' (ttgcgtaatagagtatgattag), Control Region-99 bp-3' (tagtagttcccaaaatatgac), COXI-99 bp-Biotin-5' (tcaaagtatttagctgacttg), and COXI-99 bp 3' (caactgtaaataagaaaataaagc) primers followed by gel elution. LSP-half and HSP-half ds DNAs were formed by gradual cooling from 95˚ C of Control A-half-FWD (tagtagttcccaaaatatgacttatattttagtacttgtaaaaat) with Control A-half-REV (atttttacaagtactaaaatataagtcatattttgggaactacta) and Control B-half-FWD (atcatgttccgtgaaccaaaactctaatcatactctattacgcaa) with Control B-half-REV (ttgcgtaatagagtatgattagagttttggttcacggaacatgat), respectively. All primers were HPLC purified. The pUC19 plasmid DNA (Invitrogen) used in AFM experiments was linearized by *Bam*HI restriction and gel purified.

Recombinant TFAM Protein Purification. Mature mouse TFAM GST-tagged protein was expressed from the pGEX-4T1 plasmid in BL21-AI cells (Invitrogen) according to the manufacturer's recommendations. Induced cells were lysed by digestion and sonication in lysis buffer (PBS adjusted to 300 mM NaCl and 2 mM DTT) or high-salt lysis buffer (PBS adjusted to 500 mM NaCl and 2 mM DTT), and a subsequent high-

speed supernatant was loaded onto a 1 ml Hitrap GST column via Superloop injection on an ÄKTA FPLC (GE Healthcare) at 4˚ C. After extensive washing in lysis buffer, the column was removed and injected with buffer plus Thrombin protease (GE Healthcare) and incubated at room temperature for 1 hr. The column was replaced on the FPLC followed by a benzamidine column (GE Healthcare) to remove thrombin and the unbound material was collected. Digestion was repeated up to 5 times, after which the columns were washed in the same buffer plus 50 mM GSH (Roche). In our experiments, exposure to thrombin for longer than 1 hr per incubation led to additional cleavage of a cryptic thrombin site within the first HMG box of TFAM. Columns were cleaned with 6M guanidine and then re-equilibrated with lysis buffer. The collected protein was equilibrated into lysis buffer by centrifugal concentration and contaminating GST-tagged protein and Thrombin were removed by passage through the Hitrap GST / benzamidine columns. Proteins were stored at –20 ˚C in 25 mM HEPES, pH 7.6, 150 mM NaCl, 50% glycerol, 1 mM DTT.

Computational Analysis of AFM Height Scans. All computational work was performed using custom written MATLAB 7.0 (The MathWorks) routines and the Image Processing Toolbox.

AFM images are treated as matrices of height values with elements a_{ij}, where index *i* is the row and *j* is the column. The mean value $\overline{a}$ of each image was calculated to establish a height threshold and to create a binary image containing only DNA. The threshold was set to $4\overline{a}$ and images were visually inspected to make sure that the selected pixels corresponded to the expected morphology. Using the data of all available

images of naked DNA on mica, we computed the mean DNA height ($\overline{h}_{DNA}$) and the standard deviation of the distribution (σ_{DNA}).

To identify the pixels that correspond to DNA molecules, a height threshold was set at ($\overline{h}_{DNA} - \sigma_{DNA}$). Because the pixels above the threshold also include those that correspond to irregularities on the surface and imaging noise, a morphology analysis was subsequently performed and binary images generated. First, we identified DNA objects by establishing a connectivity matrix, which was defined such that pixels above the height threshold are connected if their edges or corners touch. Second, the surface area of the biggest DNA object in the image was calculated and all the objects with areas smaller that 3% of the biggest were removed from the analysis. This effectively removed poly-lysine irregularities from the images.

To quantify protein occupancy of the DNA molecules, a second threshold was established to identify pixels for which the height of the objects is twice the value obtained for naked DNA, or $2\overline{h}_{DNA}$. The ratio between the number of pixels above this threshold and the total number of pixels of the objects was computed, yielding the Relative Protein Occupancy parameter. Hill transformation of these data was achieved by correcting for maximal binding at 100 μg/ml to θ=0.99. Proportional corrections were applied to the remaining occupancy values.

To quantify horizontal compaction on the substrate plane, we computed the ellipse that has the same normalized second central moments as the object (Haralick and Shapiro, 1992), which is the ellipse that best approximates the 2-D region described by the object. The area of a DNA molecule divided by the area of its bounding ellipse yielded the Coefficient of 2-D Compaction.

To quantify compaction in both the horizontal and vertical planes, we divided the maximum height of each DNA object by the length of the long axis of its corresponding ellipse, yielding the Coefficient of 3-D Compaction.

Surface plasmon resonance using LSP and HSP sequences. For experiments with the LSP-Half and HSP-Half ligands, native SA (Sigma) was manually immobilized to research-grade CM4 sensor chips using the Amine Coupling Kit (Biacore AB). As described above, immobilized SA was pre-conditioned and reference/active surfaces (biotinylated LSP-Half or HSP-Half oligonucleotides; 45 bp each; ~30 kDa) were prepared in a similar fashion. Kinetic analyses were performed such that TFAM was diluted in HBS-EP and injected at 25 μl/min (120 sec association + 120 sec dissociation) over the reference SA and active oligonucleotide surfaces (~25 RU). Regeneration and data analysis were as described above.

Supplemental Results

Atomic force microscopy of circular DNA reveals cooperative binding by TFAM. We observed that TFAM could compact mixed circular DNA molecules (containing both supercoiled and relaxed DNAs) (Supplementary Figure 1A). Although quantitative assessment of the compaction of circular DNA is difficult due to the compaction induced by supercoiling, we detected hallmarks of cooperative binding in the localized addition of TFAM onto the circular substrate (Supplementary Figure 1B).

Figure Legends

Supplementary Figure 1. Nanoscope atomic force microscopy imaging of TFAM binding to circular DNA. A plasmid preparation of pUC19 containing a mixture of supercoiled and relaxed circular DNA was bound by TFAM. (*A*) TFAM compacts circular DNA. (*B*) TFAM binds circular DNA with characteristics of cooperative binding. Shown are two circular DNA molecules with localized TFAM bound, one DNA molecule with more TFAM associated and greater compaction (left), the second with reduced TFAM associated and minimal compaction (right). Scale bar is 0.5 μm.

References.

Haralick, R.M. and Shapiro, L.G. (1992) *Computer and robot vision*. Addison-Wesley Pub. Co., Reading, Mass.

A.

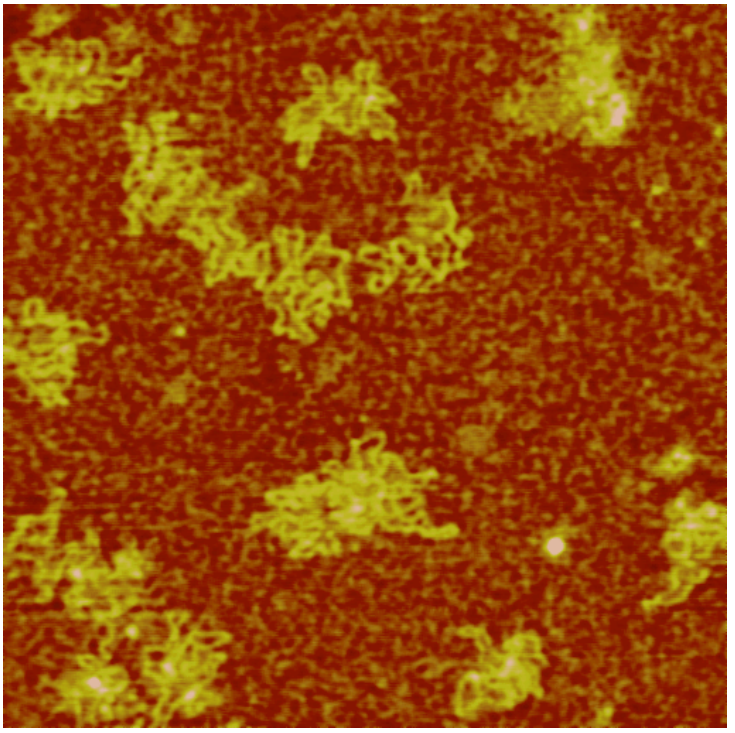

B.

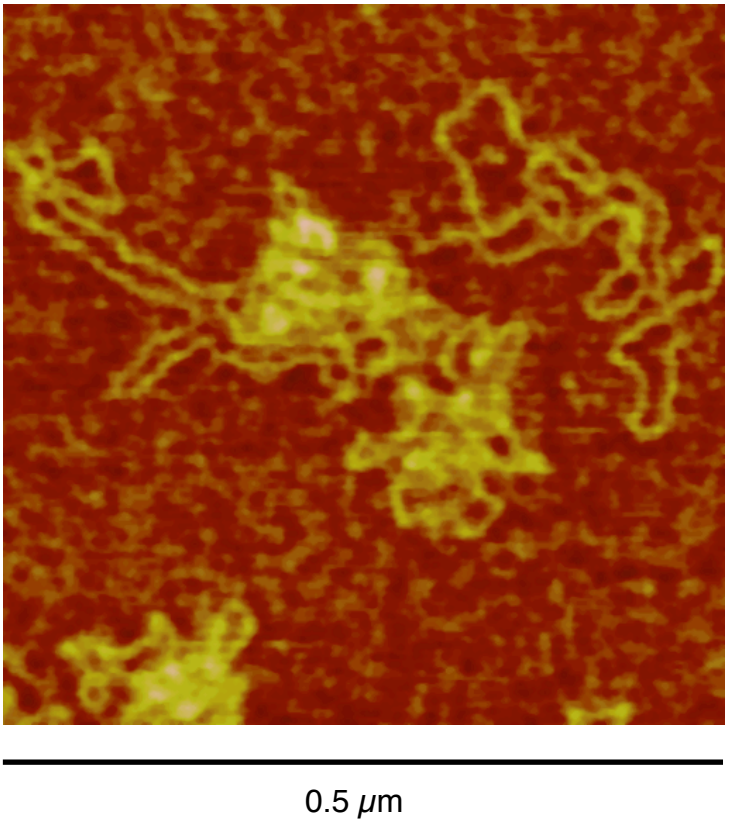

Figure S1